

^6Li and ^7Li MAS NMR and In Situ X-ray Diffraction Studies of Lithium Manganate Cathode Materials

Young Joo Lee, Francis Wang, and Clare P. Grey*

Dept. of Chemistry, State University of New York at Stony Brook, Stony Brook, NY 11794-3400

Sanjeev Mukerjee,

Dept. of Chemistry, Northeastern University, 360 Huntington Avenue, Boston, MA02115

James McBreen

Department of Applied Sciences, Brookhaven National Laboratory, Upton, NY 11793-5000

ABSTRACT

^6Li MAS NMR spectra of lithium manganese oxides with differing manganese oxidation states (LiMn_2O_4 , $\text{Li}_4\text{Mn}_5\text{O}_{12}$, $\text{Li}_2\text{Mn}_4\text{O}_9$, and $\text{Li}_2\text{Mn}_2\text{O}_4$) are presented. Improved understanding of the lithium NMR spectra of these model compounds is used to interpret the local structure of the $\text{Li}_x\text{Mn}_2\text{O}_4$ cathode materials following electrochemical Li^+ deintercalation to various charging levels. In situ x-ray diffraction patterns of the same material during charging are also reported for comparison. Evidence for two-phase behavior for $x < 0.4$ ($\text{Li}_x\text{Mn}_2\text{O}_4$) is seen by both NMR and diffraction.

RECEIVED

APR 05 1999

OSTI

INTRODUCTION

The increasing demand in the electronics industry for lightweight, compact, and high energy power sources has resulted in the study of lithium intercalation materials for electrodes in lithium ion rechargeable batteries[1]. The first commercially successful system using these lithium intercalation materials was the $\text{Li}_x\text{C}/\text{LiCoO}_2$ system[2]. However, the high cost and toxicity of Co has subsequently led to development of alternative cathode materials. The lithium manganese oxide spinel, $\text{Li}_x\text{Mn}_2\text{O}_4$, has been shown to be a promising intercalation material, meeting cost, toxicity, and efficiency criteria. However, instabilities in the cycling behavior after repeated charging and discharging processes limit the life of the cell[3, 4]. In addition, efficient lithium intercalation is not completely reproducible, suggesting that the structural properties of the materials vary with the synthesis conditions[5].

An understanding of the local structure in these materials and how this changes during charging and discharging is required in order to maximize their performance as electrodes. Diffraction studies yield long-range structural information, but do not directly provide information concerning the local order and environment of the lithium cations. ^6Li ($I=1$) and ^7Li ($I=3/2$) MAS NMR are ideal probes of lithium local environments in these complex systems.

The aim of this research is to use MAS NMR to study the local order of the lithium cations in lithium manganese oxide systems and to explore the structural and electronic properties that are responsible for the large shifts observed in these systems. The improved understanding of the lithium spectra of these materials will help in the interpretation of the local atomic and electronic structures of lithium manganate electrode materials following discharging and charging processes. Finally, these NMR studies should lead to an improved understanding of the electrochemical behavior of these materials and contribute to the development of more efficient battery materials.

EXPERIMENT

Sample Preparation

LiMn_2O_4 , $\text{Li}_2\text{Mn}_4\text{O}_9$ and $\text{Li}_4\text{Mn}_5\text{O}_{12}$ were prepared in air by solid state reaction of lithium and manganese salts (Li_2CO_3 , Mn_2O_3 and MnCO_3). The starting materials were ground together, formed into pellets and fired at different temperatures: LiMn_2O_4 is formed after firing at 850°C and $\text{Li}_2\text{Mn}_4\text{O}_9$ and $\text{Li}_4\text{Mn}_5\text{O}_{12}$ are prepared at 400°C [6]. $\text{Li}_2\text{Mn}_2\text{O}_4$ was synthesized by intercalation of LiMn_2O_4 with n-butyllithium in anhydrous hexane at 50°C for 24 hours[7].

To prepare the cathode for the electrochemical studies, LiMn_2O_4 spinel was mixed with acetylene-black, KS2 graphite, vitreous carbon fiber and poly(tetrafluoroethylene) (PTFE) binder in ethanol solvent. The mass ratio of the spinel and the other binder materials is 1:1. The composite was rolled into a sheet, dried for approximately 12 hours at 70°C , and sintered in an argon atmosphere for 1 hour at 350°C . Two cathode disks were punched out per batch. An electrochemical cell designed at Brookhaven National Laboratory (BNL) was used for the electrochemical deintercalation of lithium[8]. Lithium foil was used as the anode. 1:2M LiPF_6 in an ethylene carbonate (EC) and dimethyl carbonate (DMC) solvent mixture was used as the electrolyte. The anode and the cathode were separated by a Celgard polypropylene separator. The capacities of each sample from each batch were measured galvanostatically at a current of 0.8mA, between 3.2V and 4.5V. ^6Li enriched LiMn_2O_4 cathode was prepared for the NMR experiments with ^6Li enriched Li_2CO_3 (Isotec[®]; $^6\text{Li} > 95\%$) as the Li source. The cathode disk was then cut into small pieces. Each piece was weighed and all the pieces were fit together and placed in the same cell. The cell was charged to a specific level, disassembled (in a glove box), and one piece extracted from the cell. The cell was then reassembled, charged to another level and the process repeated. All the separate pieces of the original cathode disk (now charged to different levels) were washed with the solvent mixture to get rid of the remaining lithium-containing electrolyte and packed into the NMR rotors for the NMR experiments. The extent of lithium deintercalated (i.e., the charging level) was calculated from the weight of each piece of electrode and the measured capacity of the cathode material (determined in a separate experiment with a sample from the same batch).

Solid State MAS NMR Spectroscopy

^6Li MAS NMR spectra were acquired on a CMX-200 spectrometer with double resonance Chemagnetics probes. Single pulse and echo sequences were used with a resonance frequency for ^6Li of 29.47 MHz and $\pi/2$ pulse widths of $2.8\mu\text{s}$. All the spectra were referenced to a 1M LiCl solution, at 0 ppm.

In Situ X-ray Diffraction

In situ x-ray diffraction studies on LiMn_2O_4 were performed on the X22A beam line at the National Synchrotron Light Source at BNL. The cell assembly was specially designed for a transmission x-ray diffraction experiment. During the first charging of the electrochemical cell at a current rate of 0.65mA/cm^2 (C/10) between 3.2V and 4.4V, the (511), (333), (440), and (531) reflections were monitored at 5% charging intervals. 10.33 keV ($\lambda=1.200\text{\AA}$) x-rays were used.

RESULTS

DISCLAIMER

This report was prepared as an account of work sponsored by an agency of the United States Government. Neither the United States Government nor any agency thereof, nor any of their employees, make any warranty, express or implied, or assumes any legal liability or responsibility for the accuracy, completeness, or usefulness of any information, apparatus, product, or process disclosed, or represents that its use would not infringe privately owned rights. Reference herein to any specific commercial product, process, or service by trade name, trademark, manufacturer, or otherwise does not necessarily constitute or imply its endorsement, recommendation, or favoring by the United States Government or any agency thereof. The views and opinions of authors expressed herein do not necessarily state or reflect those of the United States Government or any agency thereof.

DISCLAIMER

**Portions of this document may be illegible
in electronic image products. Images are
produced from the best available original
document.**

⁶Li MAS NMR spectra of Li₄Mn₅O₁₂, Li₂Mn₄O₉, LiMn₂O₄ and Li₂Mn₂O₄ are shown in Figure 1. Large hyperfine shifts from the chemical shift position of diamagnetic compounds at around 0 ppm are observed for the Mn(IV) compounds, i.e., two resonances at 1980 ppm and 847 ppm are seen for Li₄Mn₅O₁₂ and one resonance at 687 ppm is observed for Li₂Mn₄O₉. Much smaller shifts are seen for the Mn(III) compound: two overlapping resonances at 101 and 118 ppm are observed in the spectrum of Li₂Mn₂O₄. The (hyperfine) shift for the LiMn₂O₄ spinel, a compound with an average Mn oxidation state Mn^{+3.5}, lies in between the Mn(III) and Mn(IV) shifts, at approx. 520 ppm. We previously assigned the resonance at 1980 ppm, observed for Li₄Mn₅O₁₂, to Li⁺ in a 16d octahedral site and the resonance at 847 ppm to Li⁺ in an 8a tetrahedral site in the spinel structure[9]. The resonance at 687 ppm (Li₂Mn₄O₉) and 520 ppm (LiMn₂O₄) are assigned to 8a sites of the spinel phase[9].

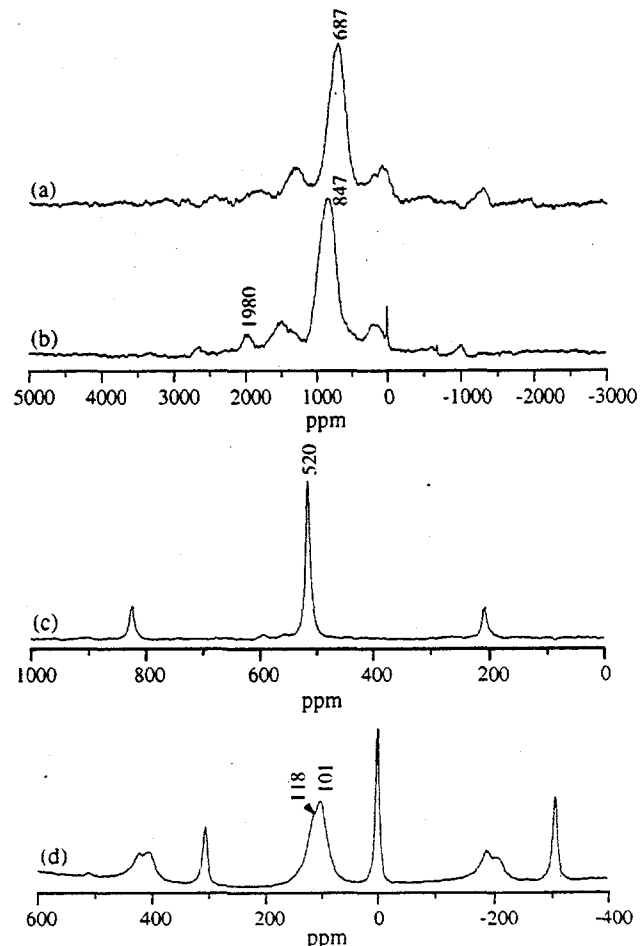


Figure 1. The ⁶Li MAS NMR spectra of (a) Li₂Mn₄O₉, (b) Li₄Mn₅O₁₂, (c) LiMn₂O₄, and (d) Li₂Mn₂O₄. (a) and (b) were acquired with a rotor-synchronized echo sequence ($\tau=1$ rotor period) with a spinning speed of ~ 21 kHz. (c) and (d) were acquired at spinning speed of 9 kHz. The isotropic resonances are marked on the spectra.

The ⁶Li NMR spectra of the spinel LiMn₂O₄ are sensitive to the synthesis conditions. ⁶Li NMR of the spinel synthesized at the lower temperature contain several resonances, indicating that there are several lithium local environments associated with the cationic defects[9]. These cationic defects are also observed in lithium excess spinels (Li_{1+δ}Mn_{2-δ}O₄) and transition metal doped materials (LiM_δMn_{2-δ}O₄, M=Cu, Cr, Zn)[10].

The NMR spectra of lithium deintercalated spinel, $\text{Li}_x\text{Mn}_2\text{O}_4$ are not consistent with the gradual removal of Li^+ and the accompanying oxidation of $\text{Mn}^{3.5+}$ to Mn^{4+} . As shown in Figure 2, the main resonance from the normal spinel phase (518 ppm at $x = 1$) shifts slowly to higher frequency and decreases in intensity while charging in the range of 0 to $\sim 50\%$. Two resonances at 525 and 645 ppm were observed in the samples charged to 70%, while only one resonance is observed at ~ 640 ppm in the highly charged samples (80 to 90%). A resonance at 930 ppm is also observed in the charged samples. The resonance at ~ 91 ppm, observed at 0% charging, is assigned to $\text{Li}_2\text{Mn}_2\text{O}_4$ that forms during the preparation of the cathode. Cathode materials prepared at lower temperatures and with less carbon do not contain this phase. Note, however, that this resonance is no longer observed (as expected) after 5% charging.

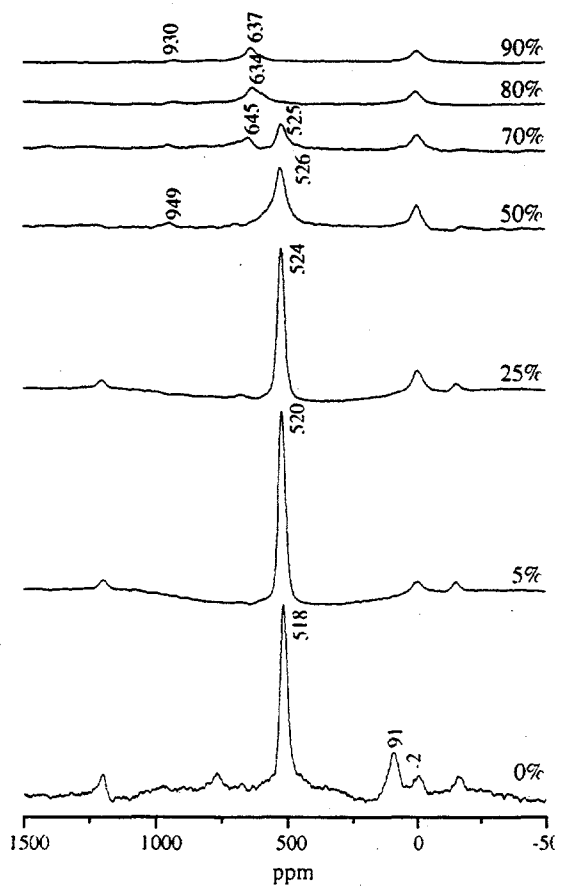


Figure 2. ${}^6\text{Li}$ MAS NMR spectra of $\text{Li}_x\text{Mn}_2\text{O}_4$ during the first charging process. The spectra were acquired with a rotor synchronized echo sequence at a spinning speed of 20 kHz. The extent of charging and isotropic resonances are indicated on the spectra.

In situ x-ray diffraction patterns obtained during the charging of $\text{Li}_x\text{Mn}_2\text{O}_4$ are shown in Figure 3. All the reflections shift to larger 2θ angles as the charging proceeds, indicating that the

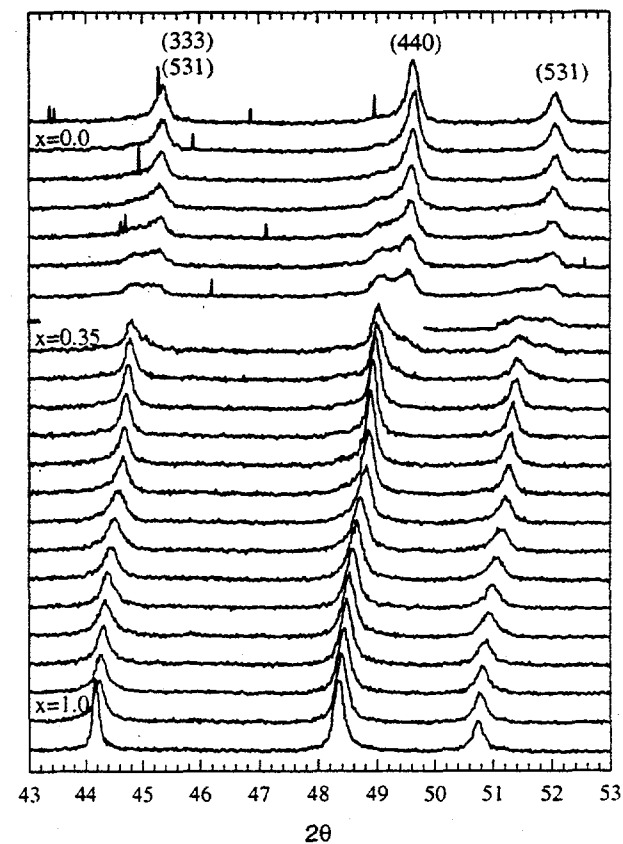


Figure 3. In situ x-ray diffraction scans showing the evolution of (511), (333), (440) and (531) Bragg peaks of $\text{Li}_x\text{Mn}_2\text{O}_4$ during the first charging cycle of the cell. Diffraction patterns are shown in intervals of $x = 0.05$, from $x = 1$ (bottom) to ~ 0 (top)

lattice parameter decreases with lithium deintercalation. No significant change in the lattice parameter of the original phase (I) is observed for $x < 0.5$, instead a second phase (II) with a smaller lattice parameter grows in. Peak splitting of all the reflections was observed in the 60 to ~ 90% charging ranges and both phases coexist. In samples charged above 90%, the diffraction lines from the original spinel phase disappear and the only the reflections from phase II remain. Similar observations have been made by earlier workers[11, 12]. Our diffraction patterns are similar to those observed by Dahn et al. [11] where two phases were also observed for $x < 0.4$. However, unlike their results, we observe a sudden change in lattice parameter between phase I and phase II. The appearance of the biphasic region for $x < 0.4$ is consistent with the NMR results where two separate resonances were observed at $x \approx 0.3$.

Comparison of diffraction and NMR results: Only very small shifts in the frequency of the ${}^6\text{Li}$ spinel resonance are observed, as the lithium is extracted from $\text{Li}_x\text{Mn}_2\text{O}_4$ in the range $x = 1.0$ to ~ 0.5, the resonance shifting from 518 to 526 ppm. This is somewhat surprising, given the sensitivity of lithium NMR to the manganese oxidation state: For example, the resonance from Li^+ cations in the tetrahedral site shifts from ~ 520 in LiMn_2O_4 to 687 (in $\text{Li}_2\text{Mn}_4\text{O}_9$) and 847 ppm (in $\text{Li}_4\text{Mn}_5\text{O}_{12}$), as the manganese oxidation state is increased from +3.5 to +4.0. Since 50% charging corresponds to an increase in the average oxidation state from +3.5 to ~ +3.75, a significant change in shift of more than 80 ppm is predicted. Any phase that does not contain lithium cations (e.g., $\lambda - \text{MnO}_2$) will not be detected by NMR. However, no evidence for a second phase is observed by diffraction in this charging range, and thus our NMR results cannot be explained by suggesting another phase is present with a high manganese oxidation state (unless this phase is amorphous). LiMn_2O_4 is a hopping semiconductor, and the size of the lithium (hyperfine) shift depends on the (unpaired) electron spin density in the d orbitals. Since only a small shift is observed, the unpaired electron spin density in the e_g orbitals near the Li^+ cations must remain very similar during the initial stages of charging. We have previously showed that lithium cations near defect sites are coordinated to higher oxidation state manganese ions (via Li-O-Mn bonds), presumably due to an increase in the energy of the Mn e_g orbitals, in comparison to energy of the e_g orbitals in the defect-free spinels. Thus we propose that the changes in manganese oxidation state occur locally, and that the Mn oxidation state does not increase uniformly over the whole sample: During the early stages of deintercalation, removal of a Li^+ cation results in an increase in the manganese oxidation state near the Li^+ vacancy. Due to an increase in the energy level of the e_g orbitals, associated with the Li^+ removal, there is no significant overall change in the electron spin density in the Mn e_g orbitals in Mn atoms coordinated to Li atoms in the Li^+ -containing regions of the crystallite. One possible explanation for these results is that as charging proceeds, Li^+ is deintercalated from regions in the sample with similar, essentially constant, manganese oxidation states. This suggestion is also consistent with the flat voltage plateau in this region. Clearly, at higher charging levels this no longer holds true and a new phase (II) is formed. The resonance of the phase II at ~ 640 ppm is consistent with lithium in a local environment surrounded by manganese ions in an oxidation state close to +4.

The intensity of the resonance at close to -2 ppm decreases in cathode materials synthesized at lower temperature and with less carbon. It increases, however, after multiple charging cycles, as does the resonance at 930 ppm. The resonance at 930 ppm is also observed in samples deintercalated chemically (with acidic solutions) and is associated with Mn^{4+} ions. The intensity of both resonances increases as the capacity of the cell fades, and these resonances appear to be associated with cell failure mechanisms/reactions.

CONCLUSION

⁶Li MAS NMR has been shown to be sensitive to the manganese oxidation states and lithium local structure. The compounds with higher manganese oxidation states show higher resonance frequencies in their ⁶Li NMR spectra. Two distinct ⁶Li resonances are observed during lithium extraction from LiMn₂O₄, indicating the presence of a two-step process involving two phases with different (local) discrete manganese oxidation states. Li⁺ is extracted from the normal spinel phase when the cell is charged from x = 1 to x = ~ 0.4 in Li_xMn₂O₄; a second phase containing manganese in a higher oxidation state (close to +4) exists for x < 0.4. This two phase behavior is also observed by diffraction. We are currently applying the above methodology to study a variety of different doped and undoped lithium manganates as a function of the charging cycle. It is hoped that the improved understanding of the deintercalation mechanisms that result from joint NMR and diffraction studies of this type will help explain mechanisms for capacity fading of the cell.

ACKNOWLEDGMENT

This research was performed under the auspices of the U.S. Department of Energy, Division of Materials Sciences, Office of Basic Energy Sciences under Contract No. DE-AC02-98CH10886.

REFERENCES

1. P. G. Bruce, *Chem. Commun.* 1817 (1997).
2. T. Nagaura and K. Tazawa, *Prog. Batteries Solar Cells* **9**, 20 (1990).
3. R. J. Gummow, A. de. Kock, and M. M. Thackeray, *Solid State Ionics* **69**, 59 (1994).
4. D. Guyomard and J. M. Tarascon, *J. Electrochem. Soc.* **139**, 937 (1992).
5. C. Masquelier, M. Tabuchi, K. Ado, R. Kanno, Y. Kobayashi, Y. Maki, O. Nakamura, and J. B. Goodenough, *J. Solid State Chem.* **123**, 255 (1996).
6. M. H. Rossouw, A. de Kock, L. A. de Picciotto, M. M. Thackeray, W. I. F. David, and R. M. Ibberson, *Mat. Res. Bull.* **25**, 173 (1990).
7. M. M. Thackeray, W. I. F. David, P. G. Bruce, and J. B. Goodenough, *Mat. Res. Bull.* **18**, 461 (1983).
8. S. Mukerjee, J. McBreen, J. J. Reilly, J. R. Johnson, G. Adzic, K. Petrov, M. P. S. Kumar, W. Zhang, and S. Srinivasan, *J. Electrochem. Soc.* **142**, 2278 (1995).
9. Y. J. Lee, F. Wang, and C. P. Grey, *J. Am. Chem. Soc.* in press (1998).
10. Y. J. Lee and C. P. Grey, Unpublished results.
11. M. N. Richard, I. Koetschau, and J. R. Dahn, *J. Electrochem. Soc.* **144**, 554 (1997).
12. S. Mukerjee, T. R. Thurston, N. M. Jisrawi, X. Q. Yang, and J. McBreen, *J. Electrochem. Soc.* **145**, 466 (1998).